Effect of sintering temperature on electrochemical performance of $LiFe_{0·4}Mn_{0·6}PO_4$/C cathode materials

Y. P. Huang[1], X. Li[2], Z. Chen[1], Y. Wu[1], Y. Chen*[3], C. J. Kuang[1] and S. X. Zhou[1]

Carbon coated $LiFe_{0·4}Mn_{0·6}PO_4$ ($LiFe_{0·4}Mn_{0·6}PO_4$/C) was synthesised using high energy ball milling and annealing processes. The starting materials of $Li_2C_2O_4$, $FeC_2O_4.2H_2O$, $MnC_2O_4.2H_2O$, $NH_4H_2PO_4$ were firstly milled for 40 h, and followed by further milling for 5 h after adding glucose solution. The milled sample was heated at different temperatures (550, 600, 650 and 700°C) for 10 h to produce $LiFe_{0·4}Mn_{0·6}PO_4$/C composites. The structure and morphology of the samples were investigated using X-ray diffraction, field emission scanning electron microscopy, and high resolution electron microscopy. The phase of samples annealed at 550 and 600°C mainly consists of olivine type $LiFePO_4$, but a small amount of Fe_2P impurity phase is formed in the samples annealed at 650 and 700°C. Electrochemical analysis results show that $LiFe_{0·4}Mn_{0·6}PO_4$/C synthesised at 600°C exhibits the best performance with the initial discharge capacity of 128 mAh g^{-1} at 0·1 C, and 109 mAh g^{-1} at 1 C after 500 cycles. The $LiFe_{0·4}Mn_{0·6}PO_4$/C exhibits excellent electrochemical properties for high energy density lithium ion batteries.

Keywords: $LiFe_{0·4}Mn_{0·6}PO_4$/C, Electrochemical properties, Sintering temperature, Cyclic voltammetry, Lithium ion battery

Introduction

Olivine type $LiFePO_4$ has been reported by Padhi *et al.*[1] in 1997 as a promising cathode material for lithium ion batteries. It can reversibly extract and insert Li ions in large amounts, with good safety thus enjoying good application prospect in the fields, such as electric vehicle, hybrid vehicle and intelligent energy storage.[1–4] As the heterogeneous of $LiFePO_4$, $LiMnPO_4$ has a higher discharge plateau (~4·1 V vs Li/Li^+),[5] thus largely improving energy density.[6] It has been determined for the olivine crystal structure in which Li^+ can only be transmitted along [010] direction in a one-dimensional manner,[7] and it has very low electron conduction, thus influencing electrochemical properties, particularly at low temperature discharge and high rate discharge. Because energy density of $LiMnPO_4$ is higher than that of $LiFePO_4$, the electronic conductivity of $LiMnPO_4$ is poorer than that of $LiFePO_4$,[8] thus limiting the large scale use of $LiMnPO_4$. During recent years, positive electrode materials of phosphate system such as $LiFe_{(1-x)}Mn_xPO_4$ have attracted wide attention.[9–12] It has been reported by Oh *et al.*[13] that the double-layer structure of $LiMn_{0·85}Fe_{0·15}PO_4$ and $LiFePO_4$ has excellent electrochemical properties and good safety performance. Von Hagen *et al.*[14] studied $LiFe_{0·5}Mn_{0·5}PO_4$ nanometre fibres prepared by electrospinning technique, and obtained the discharge capacity of about 100 mAh g^{-1} at 4 C rate. Liu *et al.*[15] prepared $LiFe_{0·6}Mn_{0·4}PO_4$/C double-layer carbon coated microspheres with high tap density, which has very high volumetric density. Thus, many studies are focused on improving $LiFe_{(1-x)}Mn_xPO_4$ electrochemical properties by keeping relatively high discharge plateau of $LiMnPO_4$ and improving the Li^+ diffusion of $LiFe_{(1-x)}Mn_xPO_4$.[16–18]

In the present paper, the $LiFe_{0·4}Mn_{0·6}PO_4$/C composite was prepared by high energy ball milling and annealing processes. The effects of sintering temperature on the structure, morphology and electrochemical properties of carbon coated $LiFe_{0·4}Mn_{0·6}PO_4$/C were studied.

Experimental

$Li_2C_2O_4$ (99+%, Alfa), $FeC_2O_4.2H_2O$ (99%, Alfa), $MnC_2O_4.2H_2O$ (Mn 30% min., Alfa), and $NH_4H_2PO_4$ (98%, Alfa) at mole ratios of $LiFe_{0·4}Mn_{0·6}PO_4$ and glucose were mixed by high energy ball milling for 40 h in a Fritsch-P5 planetary ball mill. The mixed powder was then annealed under Ar–H_2 (5%) atmosphere at 500°C for 2 h. The heated powders were dispersed in ethanol solution (100 mL). After the addition of glucose, the solution was further ball milled for another 5 h. The final slurry sample was dried at 80°C, and followed by heating at 550, 600, 650 and 700°C for 10 h under Ar–H_2 (5%) atmosphere.

The structure of samples was characterised using powder X-ray diffraction (XRD) with a D8 Discover

---

[1] Advanced Technology and Materials Co., Ltd, China Iron and Steel Research Institute Group, Beijing 100081, China
[2] College of Engineering and Applied Science, University of Cincinnati, 2901 Woodside Drive, Cincinnati, OH 45221, USA
[3] Institute for Frontier Materials, Deakin University, Waurn Ponds, Victoria 3216, Australia

*Corresponding author, email ian.chen@deakin.edu.au

Received 22 September 2013; accepted 30 January 2014
DOI 10.1179/1432891714Z.000000000664

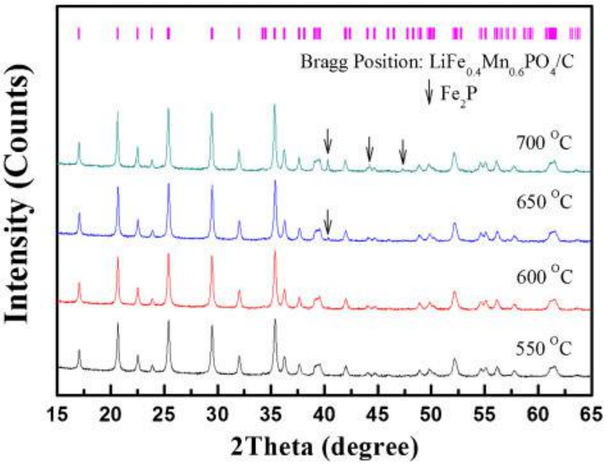

1 XRD patterns of $LiFe_{0\cdot4}Mn_{0\cdot6}PO_4$/C composites synthesised at different temperatures

diffractometer of Cu K_α radiation (λ=1·54178 Å). The morphology of sample was analysed using a scanning electron microscopy (SEM) (NOVA NanoSEM450). To study the carbon coated and the crystallinity of $LiFe_{0\cdot4}Mn_{0\cdot6}PO_4$/C, a high resolution electron microscope (JEM2010) was applied. The content of carbon was tested by a C–S analyser (CS800).

The electrochemical properties of the $LiFe_{0\cdot4}Mn_{0\cdot6}PO_4$/C electrodes were measured in CR2025 coin type cells. The working electrodes were prepared by mixing the samples, acetylene black, and poly(vinyl difluoride) at a weight ratio of 80 : 15 : 5 and pasting onto pure Al foil. Pure lithium foil was used as the counter electrode. A solution of 1M $LiPF_6$ in EC/DMC/EMC(1 : 1 : 1 by volume) was used as electrolyte. The cells were assembled in an argon filled glove box with the concentrations of moisture and oxygen below 0·5 ppm. The galvanostatic charge–discharge cycling of the assembled cells was carried out using LAND CT2001A automatic battery tester at various current rates in the voltage range of 2·0–4·5 V at room temperature. Cyclic voltammograms (CV) were recorded by using Bio-Logic VMP3 electrochemical workstation, where cyclic voltammetry test voltage ranges from 2·0 to 4·5 V.

Results and discussion

Figure 1 shows the XRD pattern taken from the final samples. After the annealing performed at 550 and 600°C, a single crystalline structure belonging to the orthorhombic Pnma group are obtained. Based on the sharp crystalline peaks in the 2θ region from 15 to 40°, sharper and narrower peaks are presented at 600 than 550°C, meaning that high crystallisation is achieved at this temperature. When the sintering temperature is at

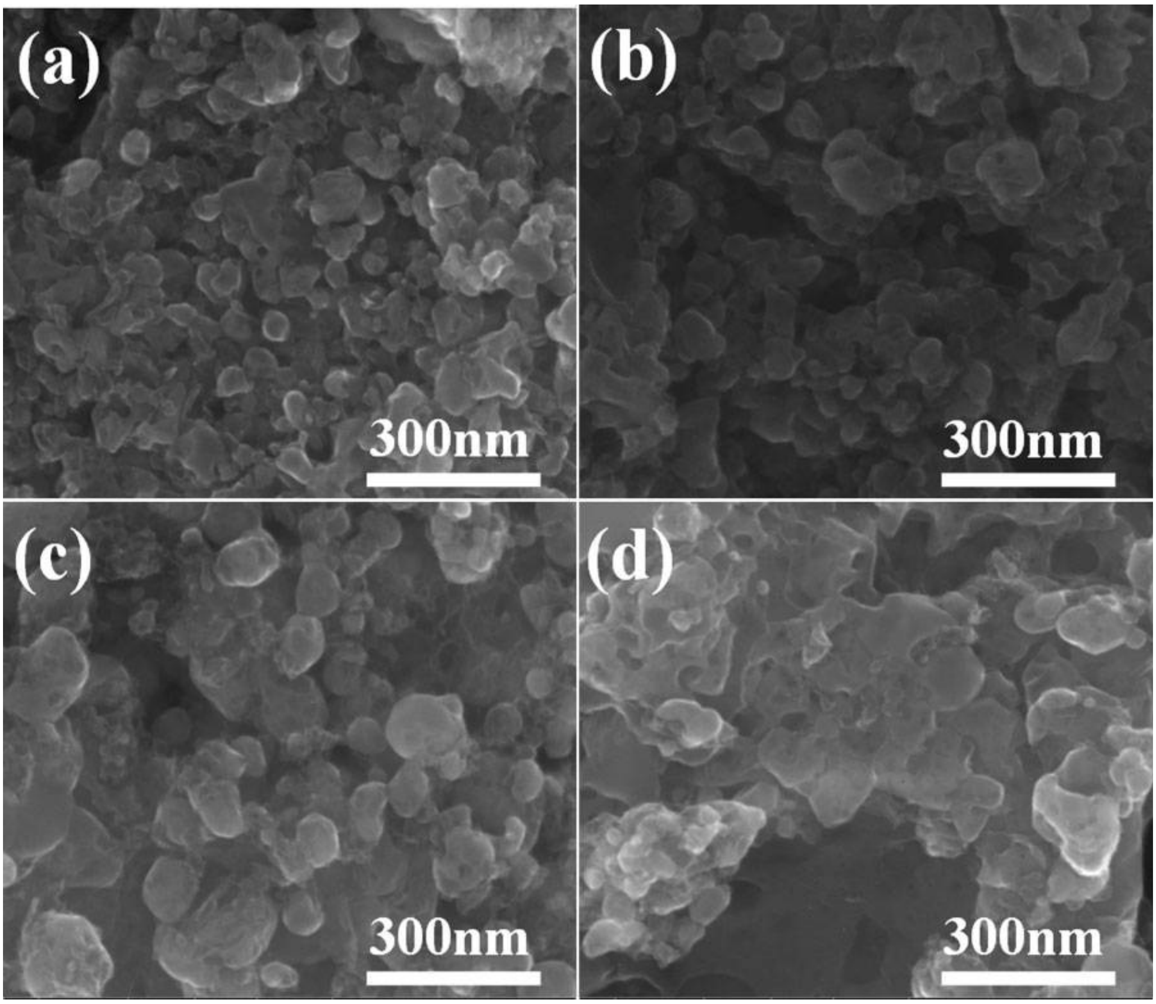

a 550°C; *b* 600°C; *c* 650°C and *d* 700°C

2 Field emission scanning electron microscopy images showing microstructures of $LiFe_{0\cdot4}Mn_{0\cdot6}PO_4$/C composites annealed at different sintering temperatures

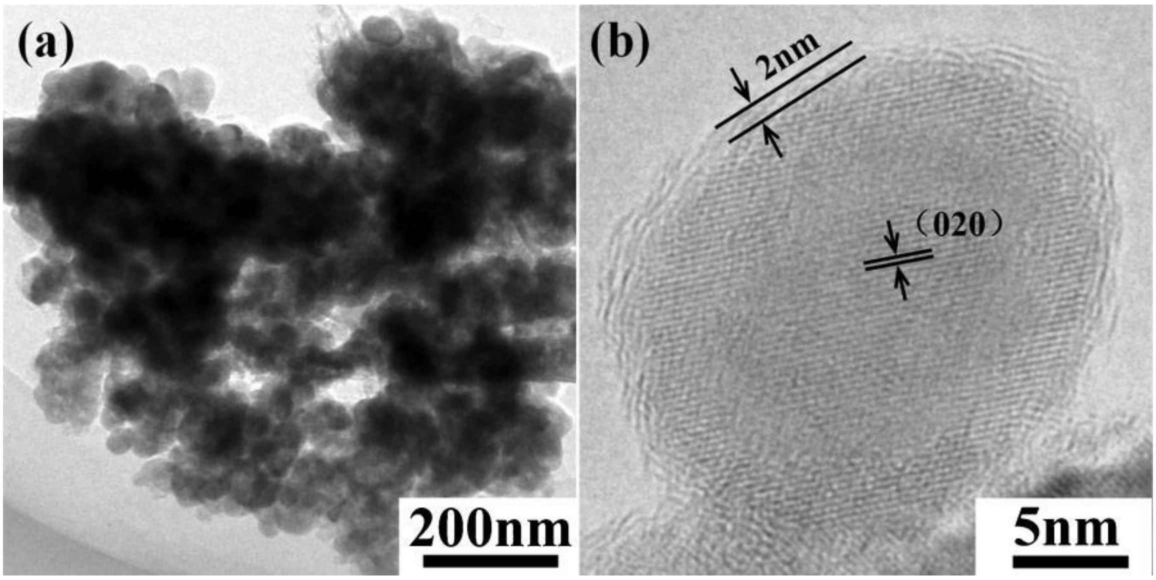

a TEM image; *b* high resolution TEM image

3 $LiFe_{0\cdot4}Mn_{0\cdot6}PO_4/C$ particle of composite annealed at 600°C

650 and 700°C, the Fe_2P parasitic phase formed. The content of C in the obtained sample about 8·5 wt-%, which is tested by C–S analyser (CS800), is too low to be detected by XRD.

Figure 2 shows SEM images of the sample morphology of clusters of 20–200 nm particles. Such clusters, composed by the particles, structure facilitates the contact between the electrolyte and electrodes, thus improving the transfer rate of the lithium ions in the materials. Increasing the synthetic temperature from 550 to 700°C, the average particle size of the composites is found to vary from about 20 to 200 nm. The distribution and thickness of the carbon coating are important factors which affect the electrochemical properties of olivine phosphates.

Figure 3 shows TEM images of $LiFe_{0\cdot4}Mn_{0\cdot6}PO_4/C$ composite annealed at 600°C. The average particle size is 30 nm (Fig. 3*a*). A uniform carbon coating layer about 2 nm thickness is covered on the surface of a $LiFe_{0\cdot4}Mn_{0\cdot6}PO_4$ particle (Fig. 3*b*), which makes an effective contribution to the electronic conductivity of olivine phosphates.

The sample of $LiFe_{0\cdot4}Mn_{0\cdot6}PO_4/C$ annealed at 600°C shows higher charge and discharge capacities at 0·1 C (define 1 C=170 mAh g^{-1}). As shown in Fig. 4, the initial discharge capacities obtained are 110, 128, 117 and 113 mAh g^{-1}, for annealed at 550, 600, 650 and 700°C, respectively. The sample of $LiFe_{0\cdot4}Mn_{0\cdot6}PO_4/C$ annealed at 550°C has the lowest discharge capacities because of the worse crystallisation, as shown in Fig. 1. When the sintering temperature is at 650 and 700°C, no electrode active Fe_2P phase occurred. This may be loss of capacity compared with the sample annealed at 600°C. Since the size of particles increases with the sintering temperature (as shown in Fig. 2), the sample of $LiFe_{0\cdot4}Mn_{0\cdot6}PO_4/C$ annealed at 600°C has the highest discharge capacities. This may imply that the nature of phase purity and crystallinity are more likely to be the factors that contributed to the better performance of $LiFe_{0\cdot4}Mn_{0\cdot6}PO_4/C$ than the size of particles.

The CV curves of the $LiFe_{0\cdot4}Mn_{0\cdot6}PO_4/C$ annealed at 600°C composite at various scan rates under the potential window of 2·0–4·5 V are illustrated in Fig. 5. Two sets of oxidation and reduction peaks typical for Fe^{3+}/Fe^{2+} and Mn^{3+}/Mn^{2+} in $LiFe_{0\cdot4}Mn_{0\cdot6}PO_4/C$ composites are obtained: Fe^{2+}/Fe^{3+} peak around 3·5 V and Mn^{2+}/Mn^{3+} peak around 4·1 V, respectively. At the same scan rate, Fe^{3+}/Fe^{2+} redox couple exhibited small

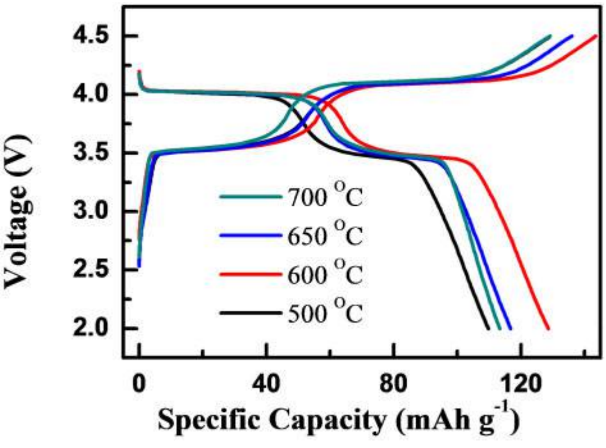

4 Initial charge–discharge profiles at 0·1 C

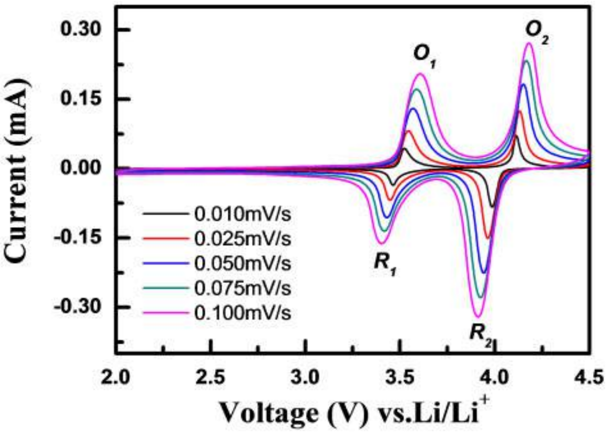

5 CV curves of $LiFe_{0\cdot4}Mn_{0\cdot6}PO_4/C$ annealed at 600°C

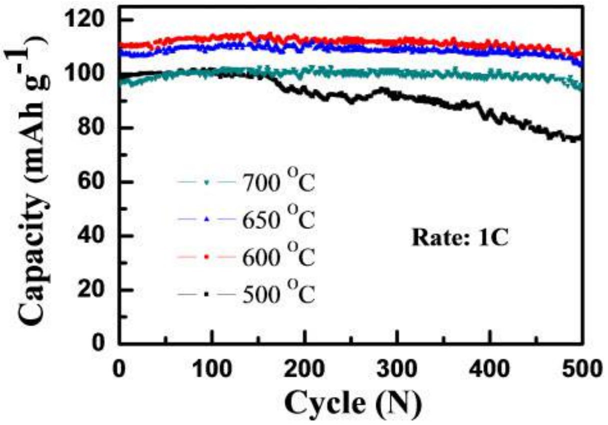

6 Cycle performance at 1 C of $LiFe_{0\cdot4}Mn_{0\cdot6}PO_4$/C composites synthesised at different sintering temperatures

peak separation than that of Mn^{3+}/Mn^{2+} redox couple. It indicated more efficient charge–transfer kinetics for Fe^{3+}/Fe^{2+} redox couple than Mn^{3+}/Mn^{2+} redox couple. Fe^{3+}/Fe^{2+} redox couple have better electrode active than that of Mn^{3+}/Mn^{2+} in $LiFe_{0\cdot4}Mn_{0\cdot6}PO_4$/C.

Figure 6 shows the 1 C rate cycling performance of the $LiFe_{0\cdot4}Mn_{0\cdot6}PO_4$/C synthesised at different sintering temperatures. At 1 C rate, the initial discharge capacities obtained are 98, 109, 107 and 96 mAh g^{-1}, for annealed at 550, 600, 650 and 700°C, respectively. Except the composite of $LiFe_{0\cdot4}Mn_{0\cdot6}PO_4$/C annealed at 550°C drastic declining, the other three composites have excellent cycling performance even after 500 cycles.

From above-mentioned results, the nanoparticle and carbon-coating are beneficial for shortening the lithium ion diffusion pathway and accelerating the electron transfer, respectively. The four olivine phosphates synthesised at 550, 600, 650 and 700°C have reasonable electrochemistry performance. Since the particle size and morphology of the four olivine phosphates are similar, the crystallinity and phase composition are key factors to affect the electrochemical properties. For the sample annealed at 600°C, a finely crystallinity and single phase olivine phosphate $LiFe_{0\cdot4}Mn_{0\cdot6}PO_4$/C composite is obtained. The average particle size is about 30 nm, and the uniform carbon layer is formed on the surface of $LiFe_{0\cdot4}Mn_{0\cdot6}PO_4$/C composite. Those contribute to the good cycle stability and electrochemical properties, making it a promising cathode material capable of delivering satisfactory performance.

Conclusions

Olivine $LiFe_{0\cdot4}Mn_{0\cdot6}PO_4$/C composite was synthesised using high energy ball milling and annealing processes. The effects of sintering temperature on the microstructure and electrochemical properties of carbon coated $LiMn_{0\cdot4}Fe_{0\cdot6}PO_4$/C were studied. The purity of phase and crystallinity of $LiFe_{0\cdot4}Mn_{0\cdot6}PO_4$ contribute to the good electrochemical performance. The $LiMn_{0\cdot4}Fe_{0\cdot6}PO_4$/C annealed at 600°C exhibits good cycle performance as cathode in lithium batteries, the initial discharge capacities are 128 and 109 mAh g^{-1} at 0·1 and 1 C after 500 cycles, respectively.

Acknowledgements

This work was supported by the ‘863’ project (Grant No. 2013AA032002), China Iron & steel Research Institute Group Foundation (Grant No. SHI11AT0540A), and Advance Technology & Materials Co., Ltd Innovation Foundation (Grant No. 2011JA01GYF).

References

1. A. K. Padhi, K. S. Nanjundaswamy and J. B. Goodenough: ‘Phospho-olivines as positive-electrode materials for rechargeable lithium batteries’, *J. Electrochem. Soc.*, 1997, **144**, (4), 1188–1194.
2. A. Yamada, S. C. Chung and K. Hinokuma: ‘Optimized $LiFePO_4$ for lithium battery cathodes’, *J. Electrochem. Soc.*, 2001, **148**, (3), A224–A229.
3. S.-Y. Chung, J. T. Bloking and Y.-M. Chiang: ‘Electronically conductive phospho-olivines as lithium storage electrodes’, *Nat. Mater.*, 2002, **1**, (2), 123–128.
4. A. Sanusi, W. J. Basirun, M. Z. Kufian and A. K. Arof: ‘Redox behaviour of crystalline $LiFePO_4$ prepared by chemical precipitation and low temperature sterilisation’, *Mater. Res. Innov.*, 2009, **13**, (3), 275–277.
5. A. Yamada, Y. Kudo and K. Y. Liu: ‘Reaction mechanism of the olivine-type $Li_{1-x}(Mn_{0\cdot6}Fe_{0\cdot4})PO_4$ (0<=x<=1)’, *J. Electrochem. Soc.*, 2001, **148**, (7), A747–A754.
6. V. Aravindan, J. Gnanaraj, Y. S. Lee and S. Madhavi: ‘$LiMnPO_4$ – A next generation cathode material for lithium-ion batteries’, *J. Mater. Chem. A*, 2013, **1A**, (11), 3518–3539.
7. S. Nishimura, G. Kobayashi, K. Ohoyama, R. Kanno, M. Yashima and A. Yamada: ‘Experimental visualization of lithium diffusion in Li_xFePO_4’, *Nat. Mater.*, 2008, **7**, (9), 707–711.
8. S. P. Ong, V. L. Chevrier and G. Ceder: ‘Comparison of small polaron migration and phase separation in olivine $LiMnPO_4$ and $LiFePO_4$ using hybrid density functional theory’, *Phys. Rev. B*, 2011, **83B**, 075112.
9. M. K. Devaraju and I. Honma: ‘Hydrothermal and solvothermal process towards development of $LiMPO_4$ (M=Fe, Mn) nanomaterials for lithium-ion batteries’, *Adv. Energy Mater.*, 2012, **2**, (3), 284–297.
10. K. Saravanan, V. Ramar, P. Balaya and J. J. Vittal: ‘$Li(Mn_xFe_{1-x})PO_4$/C (x=0·5, 0·75 and 1) nanoplates for lithium storage application’, *J. Mater. Chem.*, 2011, **21**, (38), 14925–14935.
11. L. Damen, F. De Giorgio, S. Monaco, F. Veronesi and M. Mastragostino: ‘Synthesis and characterization of carbon-coated LiMnPO4 and $LiMn_{1-x}Fe_xPO_4$ (x=0·2, 0·3) materials for lithium-ion batteries’, *J. Power Sources*, 2012, **218**, 250–253.
12. J. A. Hong, F. Wang, X. L. Wang and J. Graetz: ‘$LiFe_xMn_{1-x}PO_4$: a cathode for lithium-ion batteries’, *J. Power Sources*, 2011, **196**, (7), 3659–3663.
13. S. M. Oh, S. T. Myung, J. B. Park, B. Scrosati, K. Amine and Y. K. Sun: ‘Double-structured $LiMn_{0\cdot85}Fe_{0\cdot15}PO_4$ coordinated with $LiFePO_4$ for rechargeable lithium batteries’, *Angew. Chem.*, 2012, **124**, (8), 1889–1892.
14. R. von Hagen, H. Lorrmann, K. C. Moller and S. Mathur: ‘Electrospun $LiFe_{1-y}Mn_yPO_4$/C nanofiber composites as self-supporting cathodes in Li-ion batteries’, *Adv. Energy Mater.*, 2012, **2**, (5), 553–559.
15. W. Liu, P. Gao, Y. Y. Mi, J. T. Chen, H. H. Zhou and X. X. Zhang: ‘Fabrication of high tap density $LiFe_{0\cdot6}Mn_{0\cdot4}PO_4$/C microspheres by a double carbon coating-spray drying method for high rate lithium ion batteries’, *J. Mater. Chem. A*, 2013, **1A**, (7), 2411–2417.
16. C. A. Burba and R. Frech: ‘Local structure in the Li-ion battery cathode material $Li_{1-x}(Mn_yFe_{1-y})PO_4$ for 0<x<=1 and y=0·0, 0·5 and 1·0’, *J. Power Sources*, 2007, **172**, (2), 870–876.
17. K. Zaghib, M. Trudeau, A. Guerfi, J. Trottier, A. Mauger, R. Veillette and C. M. Julien: ‘New advanced cathode material: $LiMnPO_4$ encapsulated with $LiFePO_4$’, *J. Power Sources*, 2012, **204**, 177–181.
18. J. Molenda, W. Ojczyk, K. Swierczek, W. Zajac, F. Krok, J. Dygas and R. S. Liu: ‘Diffusional mechanism of deintercalation in $LiFe_{1-y}Mn_yPO_4$ cathode material’, *Solid State Ionics*, 2006, **177**, (26–32), 2617–2624.